

Characteristics of turbulent flow in a T-junction

Jungwoo Kim

Department of Mechanical System Design Engineering
 Seoul National University of Science and Technology
 Seoul, 139-743, Korea
 kimjw@seoultech.ac.kr

Jin-Su Kim and Jin-Ho Lee

Korea Institute of Nuclear Safety
 Daejeon, 305-338, Korea

ABSTRACT

In the present study, a large eddy simulation, at conditions of experiments by Vattenfall, was performed in order to investigate the phenomenon of turbulent mixing affecting the thermal fatigue in a T-junction. Particular attention is paid to the effect of M_R on the flow characteristics in a T-junction. To do so, two different M_R 's (0.114 and 1.04 corresponding to wall jet and impinging jet) are considered.

To investigate the turbulence characteristics related to the thermal fatigue phenomenon, the mean and rms streamwise velocity distributions are examined. Also, the frequency characteristics which are known to be one important parameter for thermal fatigue are seen. The dominant frequency scaled with the bulk property in the downstream region of the junction shows an increased trend with respect to M_R .

INTRODUCTION

The problem of thermal fatigue is frequently encountered in many thermo-hydraulic systems such as combustion engines, turbines, exhaust systems, reheat systems and so on because it plays an important role on the lifetime of pipe systems. Therefore, many studies have been conducted to understand the thermal fatigue phenomenon (Metzner and Wilke 2005).

The thermal fatigue mainly occurs in the pipe systems where two flows with different temperatures mix together. Especially, a T-junction is one of the typical components with a considerable potential of thermal fatigue (Chapuliot et al. 2005; Hu & Kazimi 2006; Lee et al. 2009). The T-junction configuration consists of two pipe systems intersected perpendicularly, and they are called main and branch pipes. In T-junction configuration the two freestreams with higher and lower temperatures mix and then induce thermal fatigue generated by the temperature change in the wall, which is known as the main source of the structural damage of T-junction. Therefore, many efforts have been done to understand how two streams in the T-junction mix.

Inside the T-junction the mixing of the main and the branch flows creates the complex turbulent structure. Previous studies (Westin et al. 2008; Walker et al. 2010)

have shown that the T-junction problem cannot be accurately predicted by RANS- or URANS-based simulation approaches. As a similar example, in terms of a jet in crossflow similar to T-junction, it has been reported that RANS calculations provides a reasonably good prediction of mean velocities but a poor prediction of turbulence intensities while LES is shown to accurately predict both the mean velocities and turbulence intensities (Muppidi & Mahesh 2007; Yuan et al. 1999; Schluter & Schonfeld 2000). On the other hand, the thermal fatigue problem is basically unsteady phenomenon so the inherent ability of DNS and LES techniques to handle temporal unsteadiness, which is different from RANS turbulence model, is also one of the main advantages in investigating the problem. Therefore, more accurate numerical simulation techniques such as DNS and LES are regarded as a promising tool to investigate the T-junction problem. In DNS, all the turbulence motions are resolved in the grid level, so if possible DNS is the best choice in predicting the given turbulence problem. However, it does not seem to be possible to take DNS approach in this study because based on the previous study (Fukushima & Fukagata 2003; $Re=10^3$, $N=570,000\sim 2,110,000$), the number of grid point required at Reynolds number of about 10^5 is to be almost 0.6~1.8 billion due to $\eta/L \approx Re^{3/4}$ (η : Kolmogorov scale, L : characteristic length scale). Therefore, between the two techniques (DNS and LES) LES is seen to be a feasible approach from a viewpoint of the current Computing power.

Therefore, in the present study, a large eddy simulation is performed to investigate the mixing phenomenon related to the turbulent flow in a T-junction. According to Hu & Kazimi (2006), the flow type considered in this study can be classified into three kinds depending on the momentum ratio of the entering flows,

$$M_R = \frac{\rho_m V_m^2 D_m \times D_b}{\rho_b V_b^2 \pi (D_b/2)^2}$$

follows:

$$\text{Wall jet} \quad M_R > 1.35,$$

$$\text{Deflecting jet} \quad 0.35 \leq M_R \leq 1.35,$$

$$\text{Impinging jet} \quad M_R < 0.35.$$

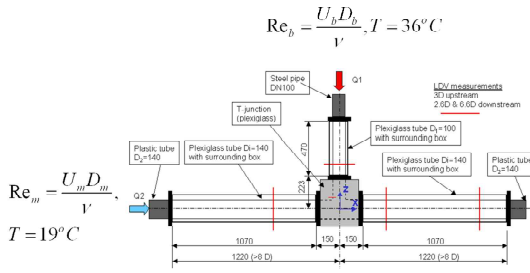


Figure 1. Vattenfall T-junction configuration. Here, subscripts m and b mean the main and branch pipes, respectively. The ratio of main and branch pipe diameter is $D_m/D_b=1.4$.

Recently, Kim and Jeong (2012) investigated the turbulence characteristics inside a T-junction for the deflecting jet case ($M_R = 1.04$), and provided useful some information on the thermal fatigue. In this study, extending Kim and Jeong's study the turbulence characteristics for the wall jet and impinging jet cases would be investigated. In Sec. 2, the problem which we would treat in this paper is described; the numerical method is outlined in Sec. 3; Sec. 4 contains results and Sec.5 a conclusion.

PROBLEM DESCRIPTION

In this section, the T-junction configuration considered in this numerical study will be described. In the present study, the T-junction configuration is taken from the experiment performed at Vattenfall Research and Development Laboratory at Alvkärlävy, Sweden (Smith et al. 2013). The details of the T-junction configuration are given as shown in Fig. 1.

According to Hirota et al. (2008), the velocity distributions measured under the isothermal condition agreed with those obtained with $T_h=60^\circ\text{C}$ and $T_c=12^\circ\text{C}$, suggesting that the buoyancy effect on the mixing is negligibly small. The temperature difference reported in the Vattenfall experiment is less than that in Hirota et al. (2008). So, the buoyancy effect could be considered to be negligible.

NUMERICAL DETAILS

The governing equations considered in this study are as below.

$$\frac{\partial \bar{u}_i}{\partial x_i} - q = 0, \quad (1)$$

$$\frac{\partial \bar{u}_i}{\partial t} + \frac{\partial \bar{u}_i \bar{u}_j}{\partial x_j} = -\frac{1}{\rho} \frac{\partial \bar{p}}{\partial x_i} + \nu \frac{\partial^2 \bar{u}_i}{\partial x_j \partial x_j} - \frac{\partial \tau_{ij}}{\partial x_j} + f_i, \quad (2)$$

$$\frac{\partial \bar{\theta}}{\partial t} + \frac{\partial \bar{u}_j \bar{\theta}}{\partial x_j} = \kappa \frac{\partial^2 \bar{\theta}}{\partial x_j \partial x_j} - \frac{\partial q_j}{\partial x_j} + h, \quad (3)$$

where \bar{u}_i , \bar{p} and $\bar{\theta}$ are the filtered velocity component, filtered pressure and filtered temperature, and τ_{ij} and q_j are the subgrid-scale stress and subgrid-scale heat flux which should be modeled by using subgrid-scale model

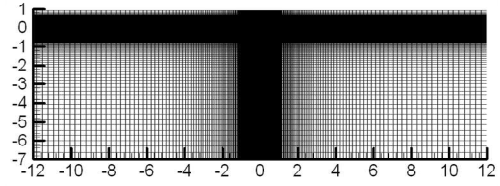


Figure 2. Grid system used in this study.

(SGS model). In Eqs. (1)-(3), the temperature field is treated as the passive scalar. This separation of the velocity and temperature fields taken in this study is supported by the result of Hirota et al. (2008) mentioned in the above.

In Eqs. (1) and (2), f_i and q are the momentum forcing and mass source/sink. Also, h is the heat source/sink. They appear in the governing equations considered because the immersed boundary (IB) method developed by Kim et al. (2001) and Kim and Choi (2004) is taken in this study to efficiently represent T-junction in a simple Cartesian mesh. The IB method is known to have advantages in mesh generation and computational time efficiency as compared to the unstructured grid approach because it can handle complex geometry in framework of Cartesian grid. The applicability and accuracy of the IB method to turbulent flows in various geometries have been validated in Park et al. (2006) and so on. The method of determining f_i , q , and h is fully described in Kim et al. (2001) and Kim and Choi (2004).

In the LES, large energy-carrying structures are directly calculated while the smaller scales are modeled with a subgrid-scale model. In the present study the dynamic Vreman model (DVM) is adopted as the SGS model which is recently developed (Park et al. 2006). Also, for the temperature, the SGS model developed by Lee and Choi (2012) is taken. The performance of subgrid-scale models used in the present study has been confirmed by *a priori* and *a posteriori* tests for various turbulence flows (e.g. forced isotropic turbulence, turbulent channel flow, flows over a circular cylinder and a sphere; see Park et al. 2006, and Lee and Choi 2012).

The basic computational details for this study are as follows. The time integration scheme considered in this study is based on the fractional step method, and is composed of the second-order accurate Crank-Nicolson method for the diffusion terms in the momentum and energy equations and third-order accurate Runge-Kutta method for the convection terms in their equations. As a result, Eqs. (1)-(3) are discretized as below.

$$\frac{\hat{u}_i^k - u_i^{k-1}}{\Delta t} = \frac{\alpha_k}{\text{Re}} L(\hat{u}_i^k + u_i^{k-1}) + 2\alpha_k \frac{\partial}{\partial x_j} (v_T (\frac{\partial u_i^{k-1}}{\partial x_j} + \frac{\partial u_j^{k-1}}{\partial x_i})) - 2\alpha_k \frac{\partial p^{k-1}}{\partial x_i} - \gamma_k N(u_i^{k-1}) - \rho_k N(u_i^{k-2}) + f_i^k, \quad (6)$$

$$\frac{\partial^2 \phi^k}{\partial x_i \partial x_i} = \frac{1}{2\alpha_k \Delta t} (\frac{\partial \hat{u}_i^k}{\partial x_i} - q^k), \quad (7)$$

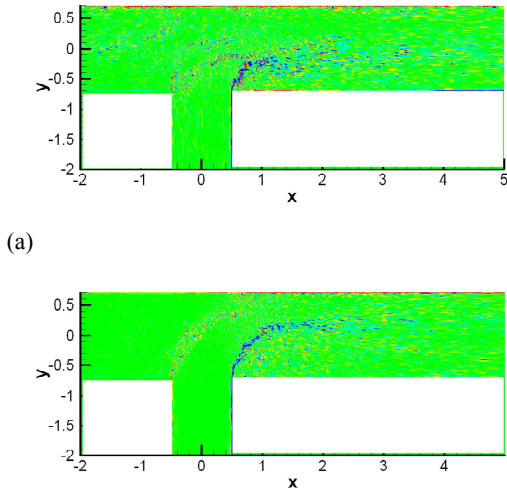


Figure 3. Instantaneous spanwise vorticity contours on x-y plane: (a) wall jet; (b) impinging jet.

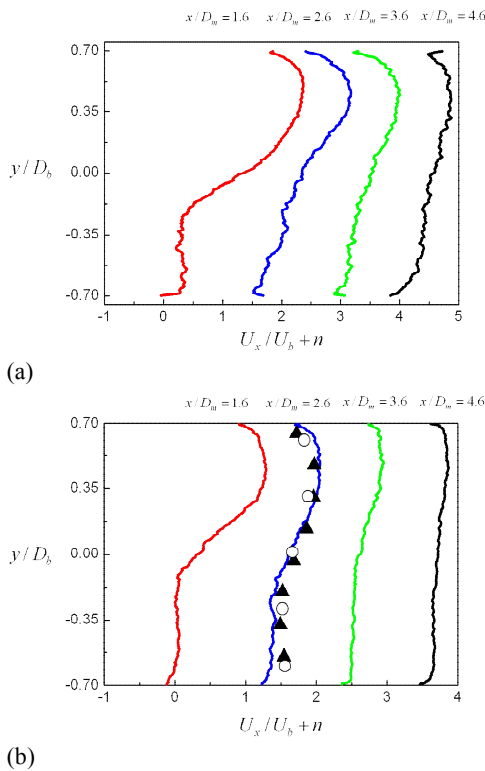


Figure 4. Time-averaged streamwise velocity at some downstream locations: (a) wall jet; (b) impinging jet. Open circle; Kuczaj et al. (2010), Solid triangle; Westin et al. (2008).

$$u_i^k = \hat{u}_i^k - 2\alpha_k \Delta t \frac{\partial \phi^k}{\partial x_i}, \quad (8)$$

$$p^k = p^{k-1} + \phi^k - \frac{\alpha_k \Delta t}{\text{Re}} \frac{\partial^2 \phi^k}{\partial x_j \partial x_j}, \quad (9)$$

where $L() = \partial^2() / \partial x_j \partial x_j$, $N() = \partial u_j() / \partial x_j$, \hat{u}_i is the intermediate velocity, ϕ is the pseudo-pressure, Δt and

k are the computational time step and substep's index, respectively. Here, f_i and q are defined inside the immersed body or on the cell containing the immersed boundary, and zero elsewhere. The grid points for the momentum forcing are located in a staggered fashion like the velocity components defined on a staggered grid. Also, the grid points for the mass source/sink are located at the cell centers like the pressure.

Figure 2 shows the grid systems used in the present study. The number of the total grid points used in this study is approximately 15 million and the fluid region consists of approximately 9 million grid points. The grids are clustered near the pipe wall. In terms of the velocity boundary condition, simple Dirichlet type of uniform velocity profile is taken as the inlet boundary conditions for main and branch pipes. Also, The convective boundary condition is taken as the outlet boundary condition.

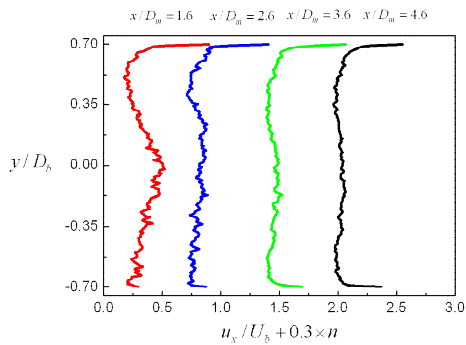
In this study, we consider the wall jet and impinging jet cases with the ratio of bulk velocities from main and branch pipes (U_m / U_b) of 1.02 and 0.255, respectively.

Each value corresponds to $M_R = 1.04$ and $M_R = 0.114$. Also, the Reynolds number based on the diameter and velocity in the branch pipe is 150,000 for both the cases.

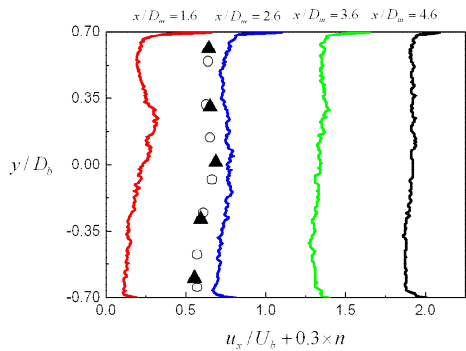
NUMERICAL RESULTS

Figure 3 shows the instantaneous spanwise vorticity contours (z-component vorticity) for wall jet and impinging jet cases considered in this study. The coordinate adopted in this study is shown in Fig. 1. As shown in Fig. 3, near the junction two streams from the main and branch pipes are strongly interacted. As a result, complicated three-dimensional vortical structures exist downstream of the junction. The details of the interaction between the main and branch pipe streams differ from the wall jet and impinging jet. In the wall jet, due to relatively strong main pipe stream the vortical structures from the branch pipe move almost along the lower side as shown in Fig. 3(a). On the other hand, in the impinging jet, the vortical structures in the front side of the branch pipe stream impinge on the upper wall of the main pipe as shown in Fig. 3(b). Therefore, it is expected that the turbulence statistics in the lower and upper sides exhibit a different behavior in the wall jet and impinging jet.

Figures 4 and 5 show the time-averaged streamwise component (x-directional) velocity profiles and rms streamwise velocity fluctuations, respectively, at four different downstream locations from the junction. To assess the accuracy of the present numerical simulation, the previous data are also included (Kuczaj et al. 2010 for numerical study, Westin et al. 2008 for experimental one). As shown in Figs. 4 and 5, the present results reasonably show good agreement with the previous data. As expected in Fig. 3, the details of the turbulence statistics are different with respect to M_R . More discussion on the difference between two cases would be done later.



(a)



(b)

Figure 5. RMS streamwise velocity fluctuations at some downstream locations: (a) wall jet; (b) impinging jet. Open circle; Kuczaj et al. (2010), Solid triangle; Westin et al. (2008).

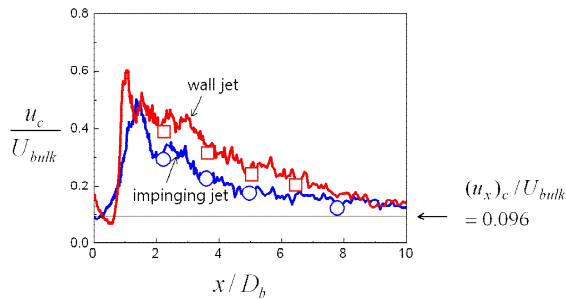
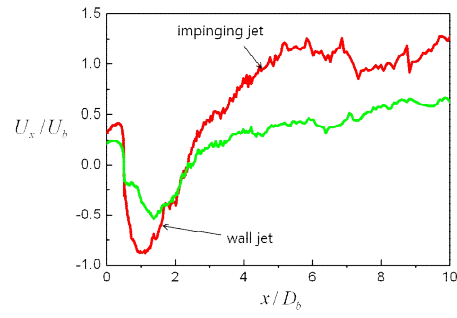


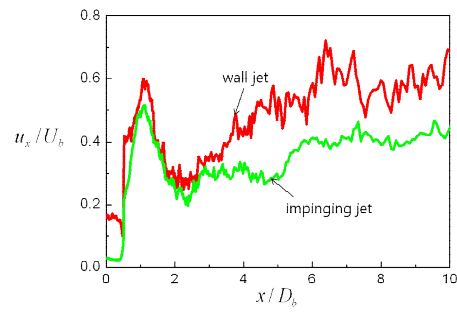
Figure 6. Distributions of rms streamwise velocity fluctuations along the centerline of main pipe. Open square; Frank et al. (2010), Open circle; Kuczaj and Komen (2010).

Although near the junction the flow is quite different from the turbulent pipe flow, one can reasonably expect that far downstream of the junction the flow could recover the turbulent pipe flow. To investigate how the turbulence in the T-junction approaches into the fully-developed turbulent pipe flow, the variation of the rms streamwise velocity fluctuations along the centerline are presented in Fig. 6. For comparison, the value reported by Wu & Moin (2008) in their turbulent pipe simulation at $Re=74,000$ is included. Figure 6 shows that although the near evolution of the flow in the T-junction is different with respect to M_R , the flow is seen to recover the fully-developed turbulent flow beyond $x/D_b \sim 10$ ($x/D_m \sim 8$).

To understand the near-wall turbulence characteristics related to the thermal fatigue, time-averaged streamwise

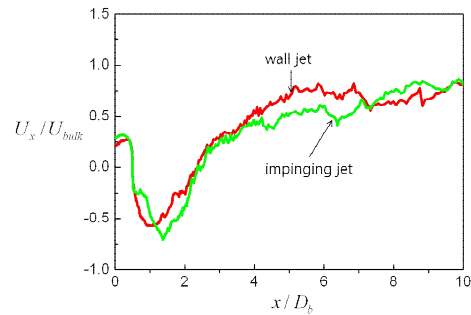


(a)

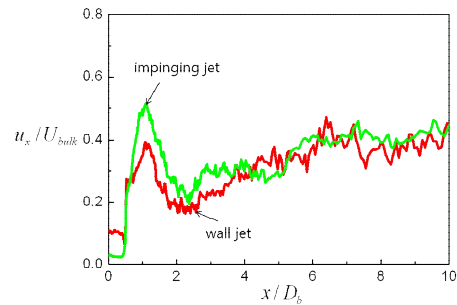


(b)

Figure 7. Distributions of (a) time-averaged streamwise velocity and (b) rms streamwise velocity fluctuations along streamwise direction at $y=-0.698D_b$. The velocity and velocity fluctuations are normalized with U_b .



(a)



(b)

Figure 8. Distributions of (a) time-averaged streamwise velocity and (b) rms streamwise velocity fluctuations along streamwise direction at $y=-0.698D_b$. The velocity and velocity fluctuations are normalized with U_{bulk} .

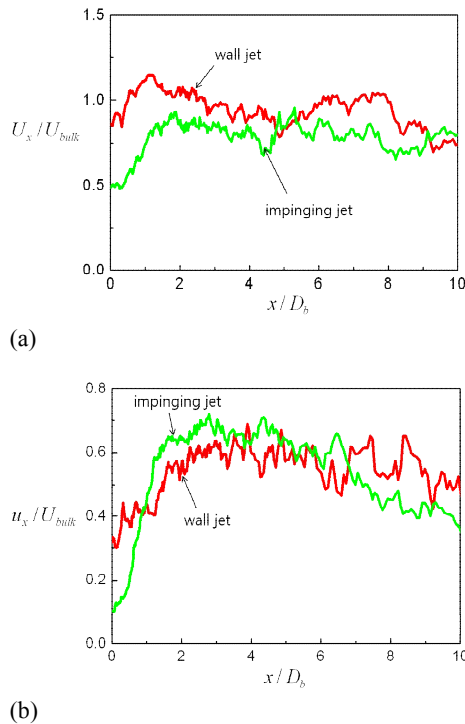


Figure 9. Distributions of (a) time-averaged streamwise velocity and (b) rms streamwise velocity fluctuations along streamwise direction at $y=0.698D_b$. The velocity and velocity fluctuations are normalized with U_{bulk} .

velocity and rms streamwise velocity fluctuations at $y=-0.698D_b$ (near the lower side) are shown in Figs. 7 and 8. The data shown in Figs. 7 and 8 are normalized with the velocity of branch pipe (U_b) and bulk velocity in the downstream region of the junction (U_{bulk}), respectively. As shown in Figs. 7 and 8, when the data are normalized with U_{bulk} , the results in the wall jet and impinging jet cases are reasonably collapsed in the downstream region. This fact is consistent with the result shown in Fig. 6. On the other hand, the negative velocities shown in Figs. 7(a) and 8(a) indicate clearly the existence of the separation bubble. The sizes of the separation bubble existing near the junction are similar in both cases. Also, in the front region of the bubble, the velocity fluctuations have their maximum value, which is consistent with the fact observed by Na and Moin (1998). The maximum is larger in the impinging jet than in the wall jet.

Figure 9 shows time-averaged streamwise velocity and rms streamwise velocity fluctuations at $y=0.698D_b$ (near the upper side). As expected in Fig. 3, the flow structures originated in the front part of the stream from the branch pipe can affect the turbulence statistics in the upper side. In the impinging jet, the structures in the front part impinge on the upper wall. Therefore, the turbulence fluctuations become larger in the impinging jet as compared to those in the wall jet as shown in Fig. 9.

Based on the previous studies, the thermal fatigue is affected by the magnitude of the turbulent fluctuations as well as their temporal characteristics (Shibamoto et al. 2008). To see the temporal characteristics of the turbulence structures, the power spectra of the streamwise

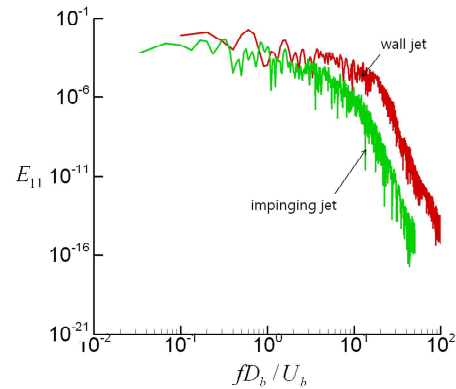


Figure 10. Power spectra of the streamwise velocity at $x=2.27D_b$, $y=-0.698D_b$ in the wall jet and impinging jet.

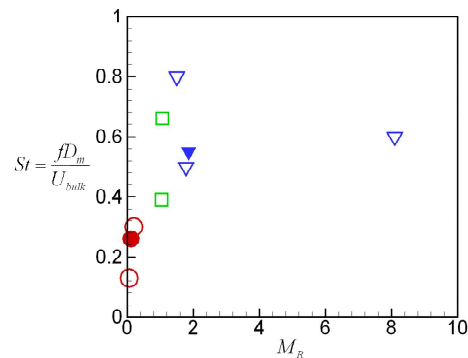


Figure 11. Variation of Strouhal number in terms of M_R : Solid circle; wall jet, Solid triangle; impinging jet. Open symbols are from previous studies. The data are obtained from Ming and Zhao (2012), Naik-Nimbalkar et al. (2010), Odemark et al. (2009) and Smith et al. (2013).

velocity at $x=2.27D_b$, $y=-0.698D_b$ is shown in Fig. 10. In the wall jet and impinging jet, the dominant frequencies normalized with velocity and diameter of the branch pipe are 0.15 and 0.6, respectively. When the dominant frequency is normalized with the bulk property in the downstream region of the junction, it shows an increased trend with respect to M_R as shown in Fig. 11. For reference, the previous data are also included. Also, the contribution of high frequency components to the total energy becomes larger with M_R (see Fig. 10). As a result, this study shows that in the wall jet and impinging jet, the thermal fatigue would happen in a different way.

CONCLUSIONS

In the present study, a large eddy simulation, at conditions of experiments by Vattenfall, was performed in order to investigate the phenomenon of turbulent mixing affecting the thermal fatigue in a T-junction. Particular attention is paid to the effect of M_R on the flow characteristics in a T-junction. To do so, two different M_R 's (0.114 and 1.04 corresponding to wall jet and impinging jet) are considered.

To investigate the turbulence characteristics related to the thermal fatigue phenomenon, the mean and rms

streamwise velocity distributions are examined. Also, the frequency characteristics are seen. The dominant frequency scaled with the bulk property in the downstream region of the junction shows an increased tendency with respect to M_R . As a result, this study shows that in the wall jet and impinging jet, the thermal fatigue would happen in a different way.

ACKNOWLEDGEMENT

This work was supported by the National Research Foundation of Korea (NRF) grant funded by the Korea government (MEST) (No. 2012055647).

REFERENCES

- Frank, Th., Lifante, C., Prasser, H.-M. and Menter, F., 2010, "Simulation of turbulent and thermal mixing in T-junction using URANS and scale-resolving turbulence models in ANSYS CFX", Nucl. Eng. Des., Vol. 240, pp. 2313-2328.
- Hirota, M., Kuroki, M., Nakayama, H., Asano, H. and Hirayama, S., 2008, "Promotion of turbulent thermal mixing of hot and cold airflows in T-junction", Flow Turb. Combust., Vol. 81, 321-336.
- Hu, L. and Kazimi, M., 2006, "LES benchmark study of high cycle temperature fluctuations caused by thermal striping in a mixing tee", Int. J. Heat Fluid Flow, Vol. 27, pp. 54-64.
- Kim, J. and Choi, H., 2004, "An immersed-boundary finite-volume method for simulation of heat transfer in complex geometries", KSME Int. J., Vol. 18, pp. 1026-1035.
- Kim, J. and Jeong, J. J., 2012, "Large eddy simulation of turbulent flow in a T-junction", Numer. Heat Transfer, Part A, Vol. 61, pp. 180-200.
- Kim, J., Kim, D. and Choi, H., 2001, "An immersed-boundary finite volume method for simulations of flow in complex geometries", J. Comput. Phys., Vol. 171, pp. 132-150.
- Kuczaj, A. K. and Komen, E. M. J., 2010, "An assessment of large-eddy simulation toward thermal fatigue prediction", Nucl. Tech., 170, 2-15.
- Kuczaj, A. K., Komen, E. M. J. and Loginov, M. S., 2010, "Large eddy simulation study of turbulent mixing in a T-junction", Nucl. Eng. Des., Vol. 240, pp. 2116-2122.
- Lee, J. and Choi, H., 2012, "A dynamic global subgrid-scale model for large eddy simulation of scalar transport in complex turbulent flows", J. Mech. Sci. Tech., Vol. 26, pp. 3803-3810.
- Lee, J. I., Hu, L.-W., Saha, P. and Kazimi, M. S., 2009, "Numerical analysis of thermal striping induced high cycle thermal fatigue in a mixing tee", Nucl. Eng. Des., Vol. 239, pp. 833-839.
- Metzner, K.-J. and Wilke, U., 2005, "European THERFAT project – thermal fatigue evaluation of piping system Tee-connections", Nucl. Eng. Des., Vol. 235, pp. 473-484.
- Ming, T. and Zhao, J., 2012, "Large-eddy simulation of thermal fatigue in a mixing tee", Vol. 37, pp. 93-108.
- Na, Y. and Moin, P. 1998, "Direct numerical simulation of a separated turbulent boundary layer", J. Fluid Mech., Vol. 374, pp. 379-405.
- Naik-Nimbalkar, V. S., Patwardhan, A. W., Banerjee, I., Padmakumar, G. and Vaidyanathan, G., 2010, "Thermal mixing in T-junctions", Vol. 65, pp. 5901-5911.
- Odemark, Y., Green, T. M., Angele, K., Westin, J., Alavyoon, F. and Lundstrom, S., 2009, "High-cycle thermal fatigue in mixing tees" new large-eddy simulations validated against new data obtained by PIV in the Vattenfall experiment", Proceedings of the 17th International Conference on Nuclear Engineering, July 12-16, Brussels, Belgium.
- Park, N., Lee, S., Lee, J. and Choi, H., 2006, "A dynamic subgrid-scale eddy viscosity model with a global model coefficient", Phys. Fluids, 18, 125109.
- Shibamoto, H., Kasahara, N., Morishita, M., Inoue, K., and Jimbo, M., 2008, "Research and developments of guidelines for thermal load modelling", Nucl. Eng. Des., 238, 299-309.
- Smith, B. L., Mahaffy, J. H. and Angele, K., 2013, "A CFD benchmarking exercise based on flow mixing in a T-junction", Nucl. Eng. Des., in press.
- Westin, J., Mannetje, C., Alavyoon, F., Veber, P., Andersson, L., Andersson, U., Eriksson, J., Henriksson, M. and Andersson, C., "High-cycle thermal fatigue in mixing tee. Large-eddy simulations compared to a new validation experiment", Proc. 16th Inf. Conf. on Nuclear Engineering (ICONE-16), May 11-15, 2008, Orlando, FL, USA.